

CHAPTER 1

INTRODUCTION TO RADIATION ISSUES FOR INTERNATIONAL SPACE STATION EXTRAVEHICULAR ACTIVITIES

M. R. Shavers, P. B. Saganti, J. Miller, F. A. Cucinotta

Space Radiation Health Project

NASA Johnson Space Center

Houston, Texas

INTRODUCTION TO RADIATION ISSUES FOR INTERNATIONAL SPACE STATION EXTRAVEHICULAR ACTIVITIES

The International Space Station (ISS) provides significant challenges for radiation protection of the crew due to a combination of circumstances including: the extended duration of missions for many crewmembers, the exceptionally dynamic nature of the radiation environment in ISS orbit, and the necessity for numerous planned extravehicular activities (EVA) for station construction and maintenance. Radiation protection requires accurate radiation dose measurements and precise risk modeling of the transmission of high fluxes of energetic electrons and protons through the relatively thin shielding provided by the space suits worn during EVA. Experiments and analyses have been performed due to the necessity to assure complete radiation safety for the EVA crew and thereby ensure mission success. The detailed characterization described of the material and topological properties of the ISS space suits can be used as a basis for design of space suits used in future exploration missions.

In radiation protection practices, risk from exposure to ionizing radiation is determined analytically by the level of exposure, the detrimental quality of the radiation field, the inherent radiosensitivity of the tissues or organs irradiated, and the age and gender of the person at the time of exposure. During low Earth orbit (LEO) EVA, the relatively high fluxes of low-energy electrons and protons lead to large variations in exposure of the skin, lens of the eye, and tissues in other shallow anatomical locations. The technical papers in this publication describe a number of ground-based experiments that precisely measure the thickness of the NASA extravehicular mobility unit (EMU) and Russian Zvezda Orlan-M suits using medical computerized tomography (CT) X-ray analysis, and particle accelerator experiments that measure the minimum kinetic energy required by electrons and photons to penetrate major components of the suits. These studies provide information necessary for improving the understanding of the current ISS space suits and provide insights into improved approaches for the design of future suits. This chapter begins with a summary of the dynamic ionizing radiation environment in LEO space and introduces the concepts and quantities used to quantify exposure to space radiation in LEO. The space suits used for EVA and the experimental partial human phantom are described. Subsequent chapters report results from measured charged particle fields before and after incident protons and secondary particles are transported through the space suits and into organs and tissues.

1.1 IONIZING RADIATION ENVIRONMENT AND EXPOSURES IN LOW EARTH ORBIT

The most notable difference between most occupational radiation exposures that occur on Earth and those in space is that astronauts experience a persistent low background field of radiations of mixed biological effectiveness, including energetic electrons, the high-energy heavy-ion component of galactic cosmic rays (GCR), secondary neutrons, and densely ionizing low-energy secondary ions and energy-degraded primary ions. In general, the significant sources of radiation exposure in LEO are relatively well known, and measured crew doses aboard the Space Shuttle are usually characterized in advance of the missions to within $\pm 25\%$ by computer simulations of the

transport of the GCR and trapped electron and proton environment and shielding models. Relative to exposures during intravehicular activities (IVA), exposures that occur during EVA have always been lower because of the shorter duration and deliberate timing of EVAs to minimize dose. Also, GCR exposures in LEO are not well attenuated by shielding and differences between IVA and EVA GCR doses are small. Trapped radiation exposures that occur during EVA are more difficult to predict and assess due to limitations in the accessibility of the radiation dosimetry and due to other circumstances that are apparent from the discussion, below.

Past Space Shuttle missions lasted no more than 18 days, whereas ISS crewmembers may be on orbit for 6 months or longer at the higher orbits preferred by mission planners to reduce atmospheric drag on spacecraft. ISS orbits at 51.6° with an altitude profile of 360–460 km (**Figure 1-1**). The dose rate experienced by inhabitants of ISS at the highest altitudes shown in **Figure 1-1** is approximately twice that at the lowest altitude. Albeit brief compared with the 11-year-long period of the solar activity cycle, the radiation environment experienced by a crew can change appreciably within a few minutes due to passage through the trapped particle belts or due to the dynamics associated with geomagnetospheric response to transient solar activity. Energetic GCR ions are present, are very penetrating, and dominate the cumulative exposure aboard ISS. However, in the radiation belts, high doses of protons or electrons occur behind minimal shielding.

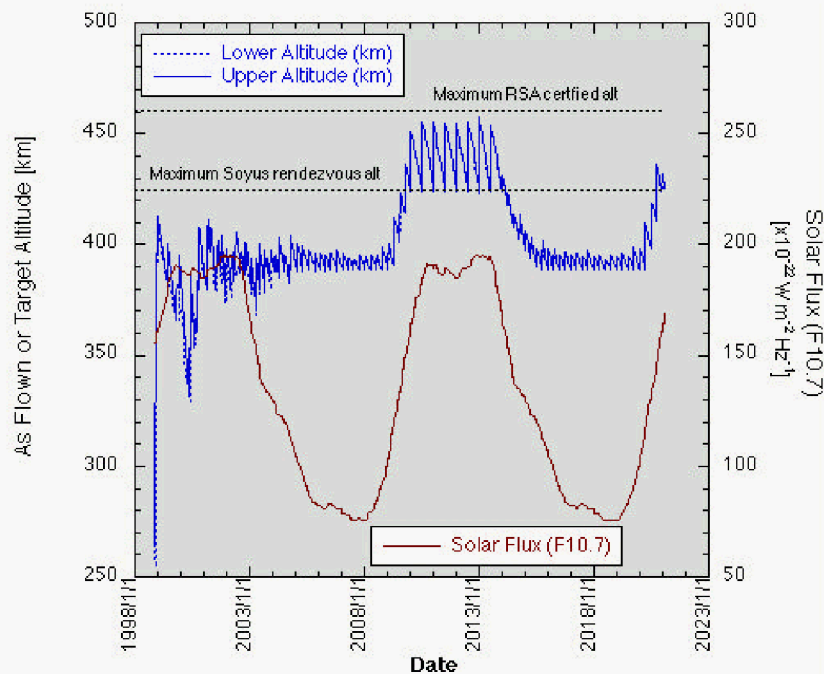


Figure 1-1. ISS altitude profile for the period 17 November 1998 through 5 May 2001. The Russian ISS segment hardware is limited to 460 km. The maximum docking altitude for the Soyuz vehicles is ~425 km.

Typical trapped proton energy spectra at ISS orbit during conditions of high and low solar activity vary in intensity by a factor of ~2, as shown in **Figure 1-2**. The intensity of the trapped proton flux is highest when solar radiation activity is lowest. The non-alignment of the Earth’s magnetic poles with the geophysical poles accounts for the well-known “anomalous” proton region above South America/Atlantic Ocean, through which several transits of trapped protons occur daily. In this region, the flux is highly anisotropic due to the azimuthal drift of the protons. The low-altitude atmosphere is denser, driving the east-west effect, and the protons are near their mirror points and

thus near 90° equatorial pitch angle. The directional difference in proton flux could be a factor of 2 to several times higher in the leading edge of the spacecraft compared to the trailing edge (Heckman and Nakano, 1965).

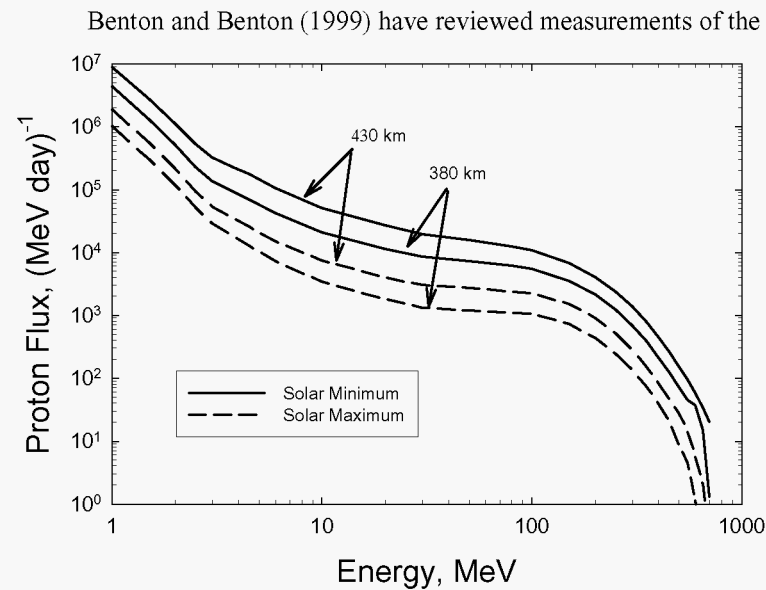


Figure 1-2. Representative trapped proton spectra for conditions typical of maximum and minimum solar activity on ISS.

include the radiation exposure accumulated during the entire mission. On a high-altitude mission, STS-61 (28.5° × 595 km), thermoluminescence radiation dosimeters (TLDs) were placed at various locations of the EVA crewmembers' bodies. The levels of uncertainties of the dosimeter measurements were too high to reveal an

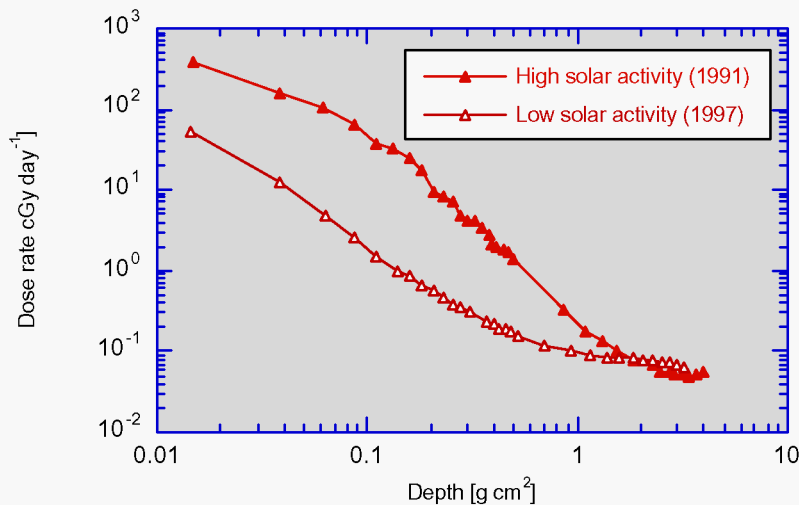


Figure 1-3. Dose rate measured by TLDs outside the *Mir* Space Station (51.65° inclination orbit × ~400 km altitude) during periods of low solar activity (1991) and high solar activity (1997).

Their data (**Figure 1-3**) indicate the absorbed dose falls off as much as 3 orders of magnitude over the first cm of penetration through the *Mir* space station. EVA dose measurements have been performed on all Space Shuttle and ISS missions. Golightly et al. (1995) compared measured doses for mission crewmembers who performed EVA and crewmembers who did not and found no statistically significant differences in absorbed dose between the paired groups. Unfortunately, those data were collected with dosimeters placed in a highly shielded location (inside the EMU and on the upper thorax under the right arm) and

increased dose associated with EVAs beyond the background exposure recorded from the IVA segments of the mission. A single set of data exists that records doses received to an astronaut and a cosmonaut exclusively during EVA (Deme et al., 1999). During low solar activity (29 April, 1997), the Hungarian Pille TLDs were worn in a pocket on the outside of the Orlan-M space suits. Measured EVA absorbed dose rates were between 60 and 80 $\mu\text{Gy hr}^{-1}$, approximately 3 to 4 times higher than the contemporaneous dose measured inside the station.

Spacecraft shielding and EVAs in low-inclination orbits have protected space inhabitants in LEO from substantial exposure to energetic electrons. With the Space Station at an orbital inclination of 51.6°, EVAs are now

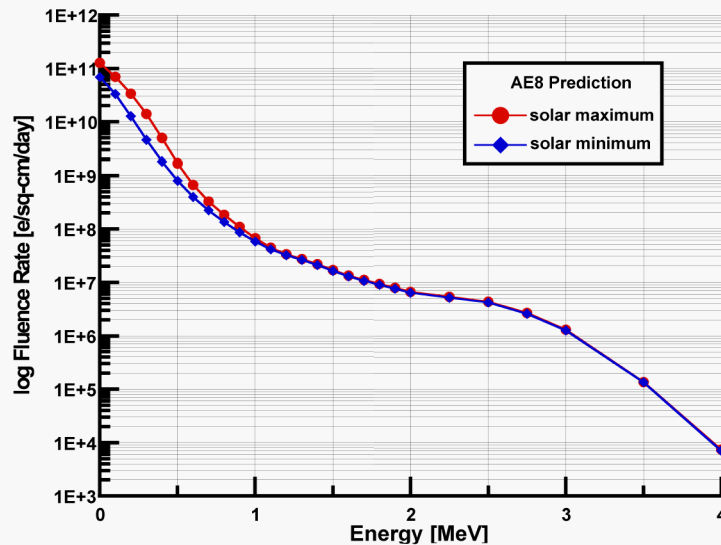


Figure 1-4. Typical trapped electron spectra for conditions of maximum and minimum solar activity. Note the increased flux during maximum solar activity. In contrast, the trapped proton flux is lower during maximum solar activity due to proton losses within the expanded atmosphere.

exposed on most orbits to “outer electron belts.” Energetic electrons will intercept ISS at high latitudes, about 20% of each orbit. A review of the CRESS satellite data indicates trapped electrons with kinetic energy as high as 30 MeV (Gussenhoven, 1996), although models generally consider only <5 MeV (inner zone) or <7 MeV (outer zone) electron populations. Typical trapped electron energy spectra at ISS orbit during conditions of high and low solar activity are shown in **Figure 1-4**.

While crewmembers inside spacecraft are well protected from the external electrons, the same is not true for those performing EVA. Unlike the more stable inner belt, the flux of trapped particles in the outer zone may change over 6 orders of magnitude in a matter of minutes (Barth 1996). High fluxes of electrons

penetrate the thin areas of the space suit and irradiate shallow tissues, such as the skin and lens of the eyes. The electron dose gradient near the surface of the body is extremely steep, decreasing by as much as three orders of magnitude within the first cm of depth, as indicated in **Figure 1-5**. For both electrons and protons, the protection an inhomogeneous space suit provides to tissues near body surfaces is difficult to determine analytically. The steep dose gradient, the inhomogeneous shielding provided by the space suit and surrounding tissues in the body, the simultaneous protracted and fractionated exposure to a changing field of mixed radiation quality, and, directionality of the ionizing field components all contribute to the problem.

Occasional exposures take place on ISS during events associated with transient solar activity. Such events added significant radiation exposure to

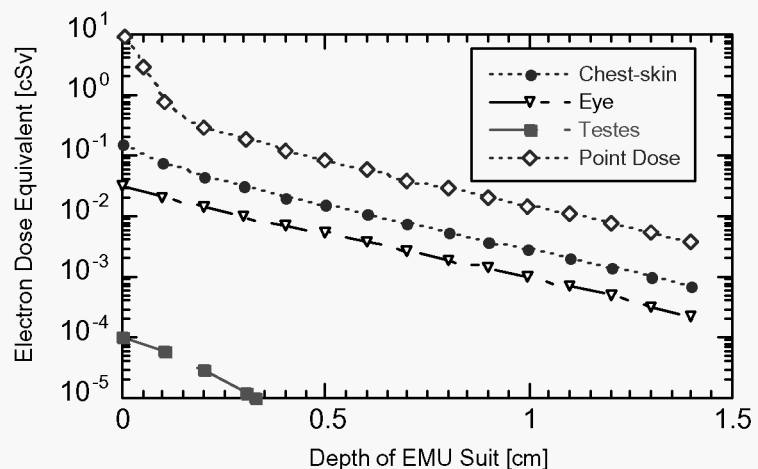


Figure 1-5. Trapped electron dose equivalent for a 6-hour-long EVA at ISS orbit estimated as a function of EMU suit thickness for an isotropic field in the worst-case orbit alignment during solar minimum activity conditions and calm geomagnetic storm conditions.

crewmembers aboard *Mir*. Severe solar particle events (SPEs) associated with solar flares directed toward Earth and that last for a period of hours or days can increase the proton dose aboard ISS with rapid onset to levels that require crewmembers to seek refuge in well-shielded locations. An example is shown in **Figure 1-6**, a plot of the proton flux above various energy thresholds measured by GOES-8 satellite during a moderate event in July 2000.

For this event, the low-energy channel is especially relevant for EVA since the threshold for proton penetration through a space suit (~ 10 MeV) is much lower than for spacecraft (~ 30 MeV). The flux of particles

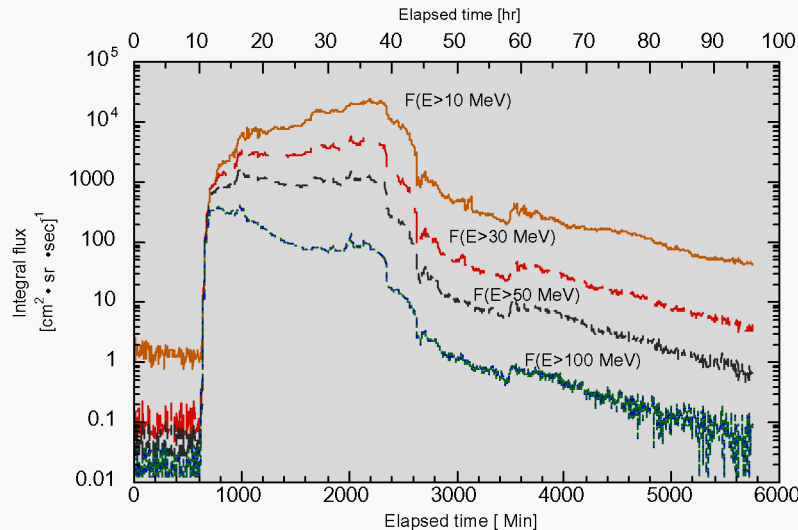


Figure 1-6. Integral proton flux spectra of the 14-17 July 2000 solar flare as measured in geosynchronous Earth orbit by the GOES-8 satellite.

below 30 MeV also continues to rise by a factor of 3 or more before peaking, while the integral flux above 30 MeV increases by about a factor of 2. High-energy protons can arrive at Earth within 10 to 90 minutes after observable manifestations appear in the solar corona at visible or X-ray wavelengths. Time-integrated energy spectra from major events observed in the past are shown in **Figure 1-7**.

Geomagnetic storms, a worldwide disturbance of the Earth's magnetic field that is distinct from regular diurnal variations, have some impact on low-altitude, low-

inclination missions. Energetic particle flux associated with the shock wave driven by a coronal mass ejection can increase suddenly by two orders of magnitude at ISS.

Such events can occur every month or even several times during a single month, and last for many days at a time. Geomagnetic disturbances (caused by coronal mass ejections of charged particles from the Sun targeted at Earth) and a severe SPE share a common cause and, occurring in coincidence, could provide a harmful dose to crewmembers. During geomagnetic storms, the protective magnetic field is compressed and higher fluxes of protons and electrons reach lower latitudes as the

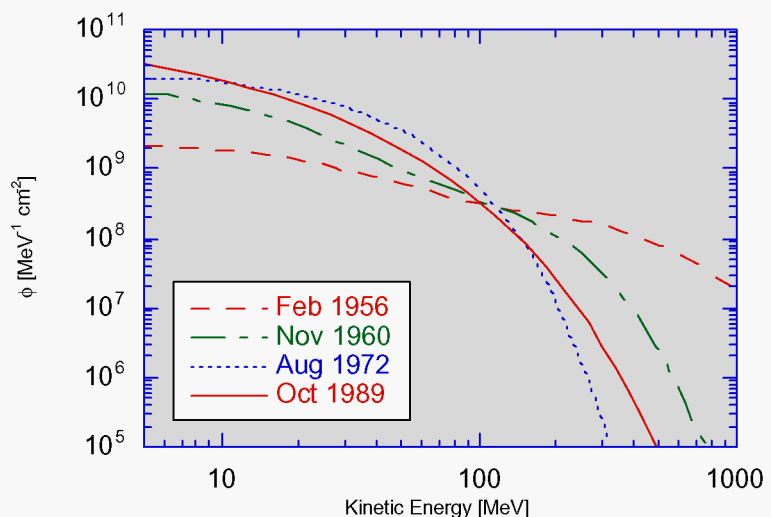


Figure 1-7. Proton energy spectra in free space for several major solar proton events.

polar-cap boundary expands. Charged particles penetrate closed field lines and can spiral along newly opened field lines to directly intercept as much as 40% of the ISS orbit. During the last two solar cycles, the probability of that occurring during a significant SPE was ~24% and was even higher during the most intense SPEs (Turner and Baker, 1998; NRC, 2000). Radiation doses to shallow (*e.g.*, skin, eye) and deep (*e.g.*, haematopoietic) tissues may significantly increase during such events, especially if commencement of an undetected storm coincides with EVA. EVA conditions aboard ISS are dangerous when the angular widths of the polar SPE zones are greater than 35° and directional proton flux is above 400 particles cm⁻²s⁻¹steradian⁻¹ (NRC, 2000). The angular width of the widened SPE zone currently is estimated using K_p as a proxy, where K_p is a 3-hr average planetary geomagnetic storm index used by space physicists. The value of K_p is determined from ground-based magnetometers in many locations throughout North America. The index value of 1 to 9 indicates current strength and geomagnetic field compression. The window of opportunity for safe EVAs is much shorter during strong magnetic storms, as indicated by the analysis of the October 1989 SPE, shown in **Figure 1-8** as estimated using the model of Wilson et al. (1991). However, additional considerations for electron belt enhancements need to be considered during times of high solar activity. Because electrons are less penetrating than solar protons, it should be possible to design space suits to minimize any impacts from trapped electrons.

The total absorbed dose from EVA results from trapped protons and electrons, GCR, and perhaps some of the “anomalous” components of galactic cosmic ions (ACR), including low-energy alpha particles and heavy ions that are completely absorbed by spacecraft, but not by EVA space suits. When interacting in matter, each of these incident

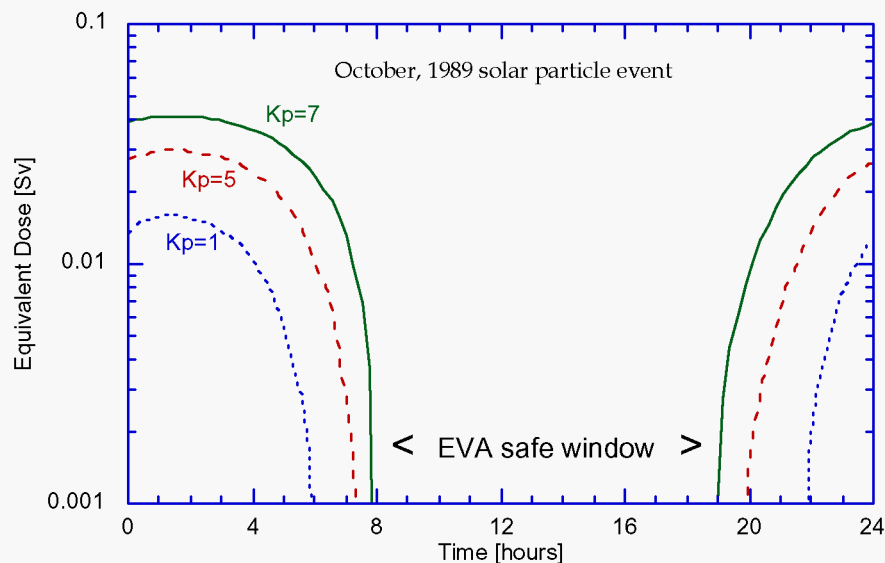


Figure 1-8. Time period when EVAs could have been safely performed on ISS during October 1989 solar particle event.

particles generates secondary radiation, including photons and secondary electrons, pions, neutrons, protons and other ions. The secondary particles can be either less or more penetrating than the incident particle, and may originate inside or outside the human body. The ACR component comprises largely singly charged photo-ionized ions of He, C, O, Ne, and Ar that have low energy and low penetrability through spacecraft. Being singly charged, they have high rigidity (thus able to penetrate

the magnetosphere to the ISS orbit) and some will penetrate a space suit. Although they are known to form trapped radiation belts, the ACR comprise less than 5% of the GCR flux of >10 MeV/A ions, and are not expected to pose a significant biological risk to astronauts (Badhwar, 2000).

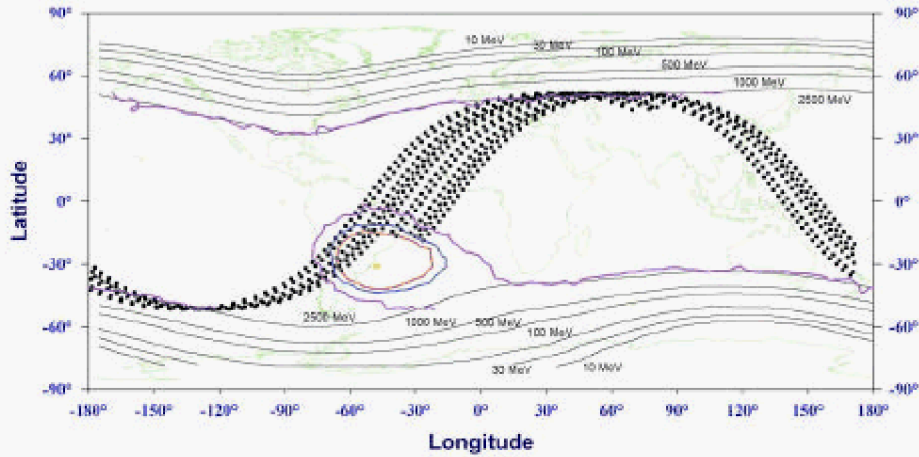


Figure 1-9. Start locations (each dot) for orbits that maintain low dose equivalent to the skin (<0.3 mSv) for ISS EVAs of 6-hr duration. Low-energy thresholds for solar protons are shown as labeled contours.

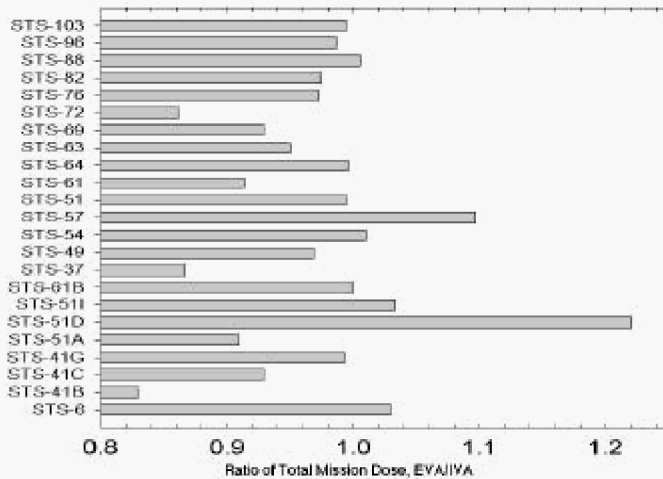


Figure 1-10. Absorbed dose ratio, EVA/IVA, for Space Shuttle astronauts. “IVA” refers to the average absorbed dose to crewmembers who remained inside the Space Shuttle during EVAs.

dosimeter outside ISS is recommended by a recent National Research Council report on radiation risks to ISS crews and is a high priority (NRC 2000).

The effectiveness of EVA timing to minimize radiation exposure is reflected in **Figure 1-10**, however limitations in EVA dosimetry need to be considered in such comparisons.

1.2 DOSIMETRIC QUANTITIES AND REGULATORY DOSE LIMITS FOR STOCHASTIC RADIATION EFFECTS

Stochastic quantities for external irradiations are expressed as equivalent dose, H_T , with units of Sv. The equivalent dose is derived by multiplying organ-absorbed dose from the radiation incident on the body, D_T [J kg^{-1} , or Gy], by the appropriate radiation weighting factor, w_R . Radiation weighting factors, given (ICRP 1991), are not

dependent on the rate of linear energy transfer (LET). In current practice, when spectral information is available for a radiation field, LET-dependent radiation quality factors, $Q(L)$, are used in place of w_R , where

$$Q(L[\text{kev} / \mu\text{m}]) = \begin{cases} 1 & L < 10 \\ 0.32L - 2.2 & 10 \leq L < 100 \\ 3000 / L & L \geq 100 \end{cases}, \quad (1)$$

as shown graphically in **Figure 1-11**. Neither w_R nor $Q(L)$ is organ-dependent; that is, the *relative* harm of the various types of radiation is considered to be the same for stochastic or deterministic biological effects (discussed below) in all organs and tissues.

The measure of detriment due to stochastic effects from non-uniform exposures is effective dose, E . Effective dose is calculated as the sum of tissue weighted H_T for all irradiated tissues or organs,

$$E = \sum_T w_T H_T, \quad (2)$$

where the tissue weighting factor w_T represents the proportionate detriment (stochastic) of tissue T when the whole body is uniformly irradiated. Effective dose incorporates stochastic risks such as nonfatal cancer, genetic risks, and relative length of life lost into the determination of w_T . Conceptually, effective dose to a tissue carries the same risk associated with a uniform whole-body exposure of the same equivalent dose. For activities in space, the National Council on Radiation Protection and Measurements (NCRP) (2000) recommends that equivalent dose should be approximated as organ dose equivalents (ICRU, 1993):

$$H_T \approx \int dV_T \int Q(L) D(L) dL, \quad (3)$$

where V_T is a volume element in tissue T and the $Q(L)$ relationship is used in place of w_R . Eqn (3) allows a more precise calculation of equivalent dose and is considered to provide an acceptable approximation for calculating effective dose, E . Large uncertainties are present in the above model of cancer risk from space radiation (Cucinotta et al., 2001a).

Career limits that are related to age at time of exposure and sex were recommended by the NCRP (2000) in Report No. 132 for space activities are given in **Table 1-1**. Although the career limits are age- and gender-specific, the ICRP (1991) determined that other factors (*e.g.*, the model used to translate risks from one population of people to another, as well as special characteristics of national populations) could be more important determinants of the relative contributions of cancer in various organs to the total cancer risk.

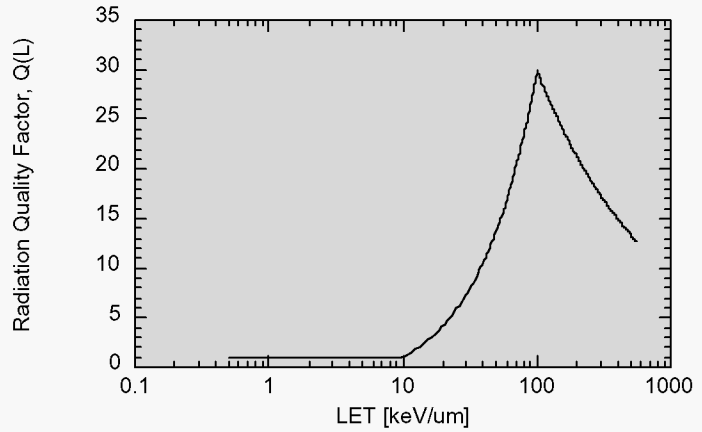


Figure 1-11. The radiation quality factor for ionizing radiation used by NASA for all space activities. Defined in Publication 60 of the ICRP (ICRP 1991).

Table 1-1. Effective Dose Limits for a Ten-Year Career Based on 3% Excess Lifetime Risk of Fatal Cancer^a

Age at Exposure	Female <i>E</i> (Sv)	Male <i>E</i> (Sv)
25	0.4	0.7
35	0.6	1.0
45	0.9	1.5
55	1.7	3.0

^aAdditional components of radiation detriment associated are discussed in text

1.2.1 Deterministic Effects

The non-stochastic or *deterministic* biological effects are those that occur with severity (not probability) that is proportionate to dose and have a presumed dose threshold for clinically significant presentation. Proposed exposure limits on non-stochastic effects are on the same order of magnitude as career doses for acute, short-term exposures. These quantities are currently under review, and are measured in terms of gray equivalents. The dosimetric quantity *gray equivalent* is calculated by multiplying the organ or tissue dose by a factor that describes the relative biological effectiveness (RBE) of a particular type of radiation. The recently proposed radiation dose limits for bone marrow, eye, and skin exposures during activities in space, shown in **Table 1-2**, are based on response thresholds for fractionated exposures. Stochastic limits on career exposure of the bone marrow are sufficiently low to prevent deterministic effects. The deterministic exposure limits values prevent deleterious responses from exposures over a single one-year period, but these limits should not be approached year after year. Recommended RBE values for deterministic effects in these tissues are independent of tissue type, and are presented in **Table 1-3**. The RBE of electrons is taken as 1.

Table 1-2. Recommended Organ Dose Limits for Deterministic Effects in People of All Ages (NCRP 2000)

	Bone Marrow (Gy-Eq)	Eye (Gy-Eq)	Skin (Gy-Eq)
Career	—	4.0	6.0
1 y	0.50	2.0	3.0
30 d	0.25	1.0	1.5

The radiation dose limits for space activities allow exposures that are higher than regulatory limits for terrestrial workers in the United States. For example, the skin limit for ground-based workers is 0.5 Sv per year, averaged over the highest exposed 1 cm² area of skin, and 0.15 Sv for the lenses of the eyes (CFR 2000). The recently proposed dose limits are based on a very limited amount of data that is relevant to exposures in space (NCRP 2000). Only EVAs that occur during extreme conditions have the potential to exceed the thresholds for these effects. The time-course of exposure is an important determinant of statistical observations of biological harm. In general, protracted and fractionated exposures to low doses of low-LET radiations (electrons and high-energy protons) are less deleterious than an acute exposure at the same dose level. This temporal effect is recognized and was included in the derivation of deterministic and stochastic dose limits for space activities.

Table 1-3. RBE Values for Determining Deterministic Dose (Gray Equivalents) From Absorbed Dose (NCRP 2000)

Radiation type	Recommended RBE	Range
Neutrons, 1 to 5 MeV	6.0	(4–8)
Neutrons, 5 to 50 MeV	3.5	(2–5)
Heavy ions (He, C, Ne, Ar)	2.5	(1–4)
Protons > 2 MeV	1.5	–

1.2.2 Environmental Monitoring, Crew Dosimetry and Alerts

Constellations of satellites (*e.g.*, SOHO, ACE, GOES, POES) monitor diagnostic solar surface conditions, the strength of the geomagnetic field, and proton and electron fluxes in geosynchronous Earth orbit and in other locations in high-Earth orbits. A system of radiation safety alert levels and response procedures are in place so that a flight director can initiate evasive actions, such as postponing EVAs and locating crew to shelter in well-shielded locations.

Radiation detectors aboard ISS include instruments that monitor the interior ionizing radiation environment and telemeter that information at regular intervals. Solid-state detectors measure the dose levels, and information about the directionality and quality of the radiation environment is collected by charged particle spectrometers. The crew passive dosimeter each crewmember wears measures that crewmember's radiation dose of record. Detectors and computer models are used to characterize the ambient radiation environment inside ISS and to report the dose equivalent to dose-limiting body organs. Each astronaut on EVA wears the same dosimeter during the entire mission and the results are read after return to Earth.

1.2.3 Radiation Dose Reduction

As previously mentioned, substantial dose reduction can be achieved by carefully scheduling EVAs to avoid trapped proton belts and the electron “horns” at high latitudes. Real-time space weather monitoring and implementation of existing flight rules greatly reduce the likelihood of dangerous radiation exposure from scheduled EVAs during SPE and/or storm conditions. Further dose reduction can be attained aboard ISS with specially designed radiation shields and the advantageous placement of onboard supplies or equipment that can contribute ancillary shielding. The directionality of penetrating trapped protons impinging on ISS can be exploited for dose reduction by shielding. The JSC Space Radiation Health Project Office's recent assessment of shielding materials with simulated space radiation environments at ground-based accelerators initiated the placement of polyethylene shielding around an ISS crew sleeping area. Future shielding enhancements, if deployed around crew quarters and pre- and post-sleep activity areas, will substantially reduce radiation doses.

For EVA, due to the low penetrability of low-energy electrons and protons, radiation dose to tissues near the body surface is determined by the minimum thickness of a space suit, and even thin amounts of additional shielding could significantly attenuate these exposures. The most effective dose-reduction strategies for EVA are scheduling EVA during benign environmental conditions, monitoring and responding to environmental conditions in real-time, and limiting total time outside.

Near-real-time evaluations of the radiation dose levels are available to crews. Pille TLD personal dosimeters can be deployed during a transient event or during EVA activities with the Orlan-M space suits outside ISS and then analyzed on orbit immediately to monitor exposures as they accumulate. New technologies are being developed to model the ambient radiation environment at any location inside or surrounding ISS and to provide the capability for a crewmember to visualize the regions of higher and lower exposure as the background radiation environment changes and spacecraft components and shielding materials are repositioned. Future crews in LEO will play an important role in monitoring and reducing their own exposure level during transient events.

1.2.4 The EMU Space Suit

The complexity of the EMU is apparent from **Figures 1-12 to 1-15**. On Earth, an EMU weighs approximately 127.3 kg (280 lb). Modular components include 11 space suit assembly items and 7 major life support system components that sustain life in a hostile environment that includes a near vacuum with rapid and severe ambient temperature gradients, intense ultraviolet radiation exposure, and the possibility of a micrometeoroid or orbital debris strike.

Anderson et al., in Chapter 9, provide the material composition and thickness of major subsystems of the EMU. Most individual layers of fabric material are homogenous, if not uniformly thick, and some have moving parts. Requirements for flexibility limit the mass and internal pressure (4.3 psid or 29.6 kPa) of the suit, yet substantial quantities of aluminum and heavier metal (poor space radiation shields) are present (Anon, 1999; 2000).

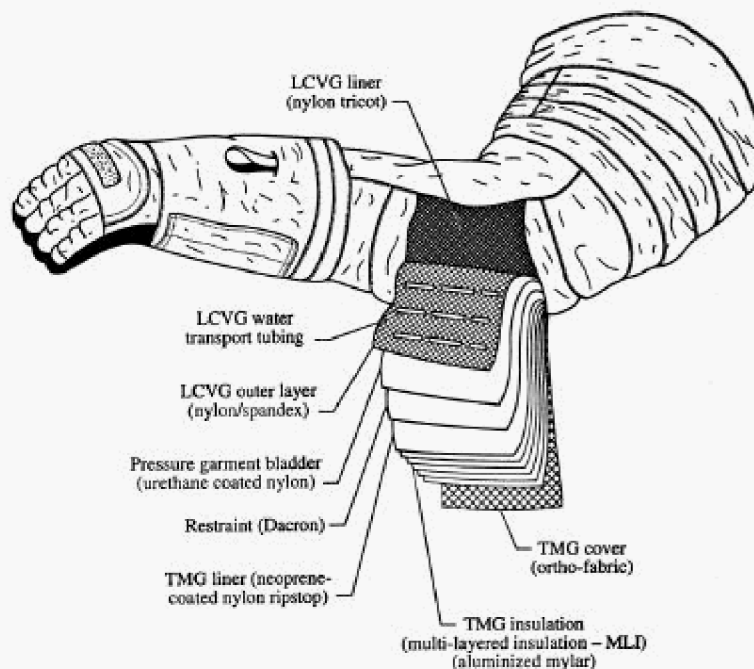


Figure 1-12. Fabric material layout used for the arms and legs of the EMU. The inner liquid-cooling and ventilation garment, also shown, is a non-homogenous fabric covering the torso and limbs that supports small water-transport tubes for regulating body temperature. (Reproduced with permission from Hamilton Sundstrand.)

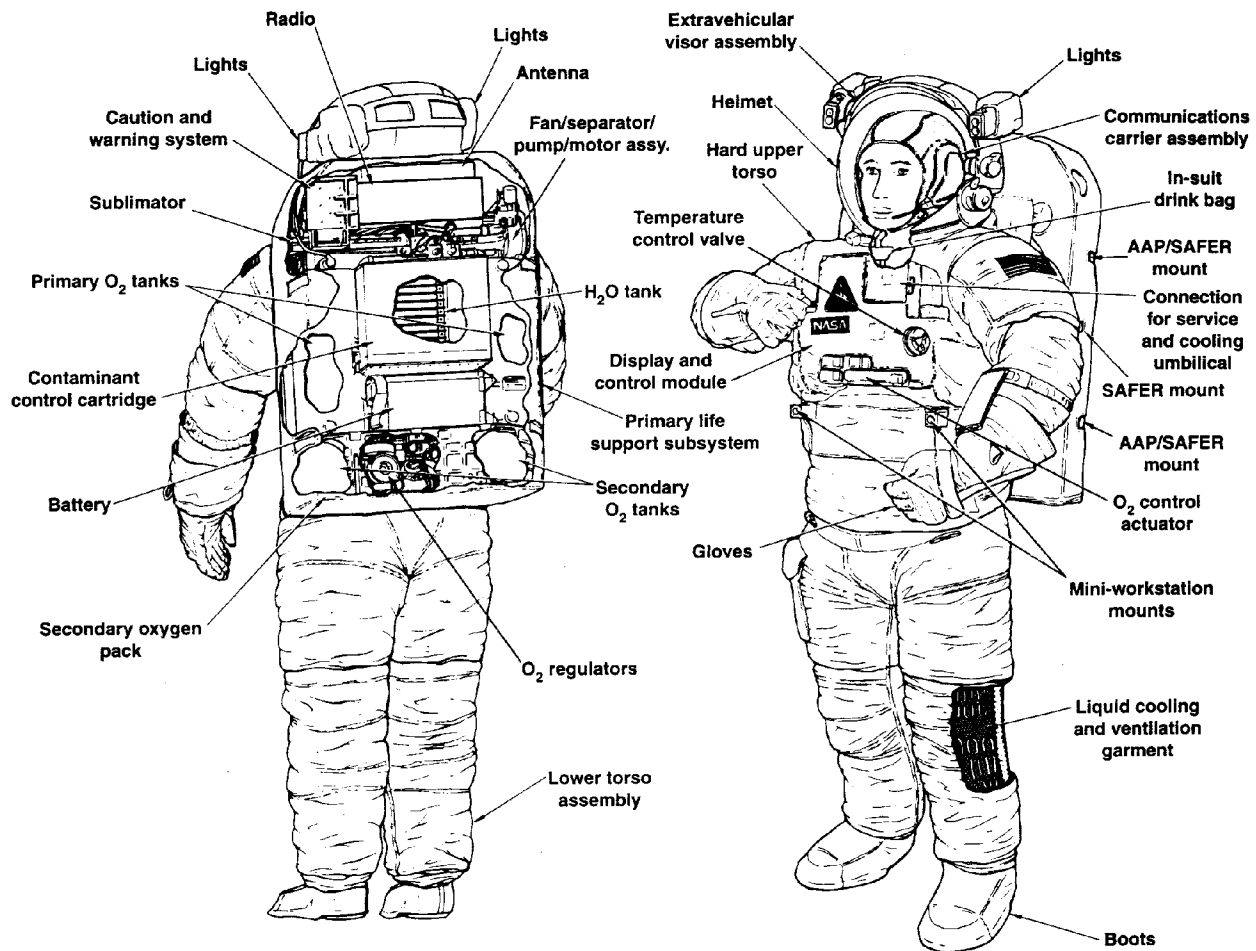


Figure 1-13. Major components of the EMU space suit assembly and life support system.
(Reproduced with permission from Hamilton Sundstrand.)

1.2.5 EMU Hard Upper Torso (HUT)

The HUT provides the structural mounting interface for the primary life support subsystem backpack (PLSS), the display and controls module mounted on the chest, the helmet, arms, lower torso assembly and the EMU electrical harness. The rigid fiberglass hard torso shell is the main component of the fabric-covered HUT. Many metallic components are present, as well, and their presence influences the radiation field transported through the suit and complicates experimental analysis and modeling. The helmet attaches to the HUT shell with the metallic neck ring and the lower torso assembly is mounted to the HUT shell with the metallic body seal closure. Additional metal hardware provides for fluid passages from the PLSS to the DCM and to the liquid cooling and ventilation garment (LCVG). Of particular significance is the metallic LCVG side of the multiple water connector (MWC), which mates cooling water line and body gas vent tubes. The metal body seal closure mounts provide the HUT with external interfaces to the mini-work station and the modified mini-work station outside the chest of the suit. The MWC and other metallic components are visible in **Figure 1-14**.

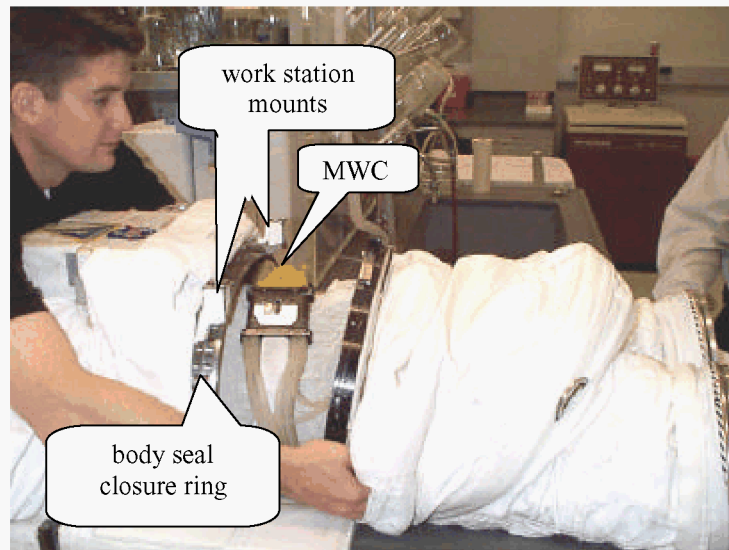


Figure 1-14. Mating of the EMU hard upper torso (left) with the lower torso assembly (right). The metallic LCVG coupling of the multiple water connector (MWC) “buckle” is visible between the torso sections, and the metal workstation mounts are visible on the metallic Body Seal Closure ring of the HUT.

1.2.6 EMU Helmet

The EMU helmet and extravehicular visor assembly (EVVA) (**Figure 1-15**) protects the lenses of the eyes from photochemical damage caused by ambient ultraviolet photons (320 to 400 nm UV-A), and protects the cornea from shorter wavelength UV-B and UV-C. The retina and cornea are also protected from potential damage from intense visible, infrared, radio frequency, and microwave exposures. The EVVA is important for reducing cataract risk (Cucinotta et al., 2001b).

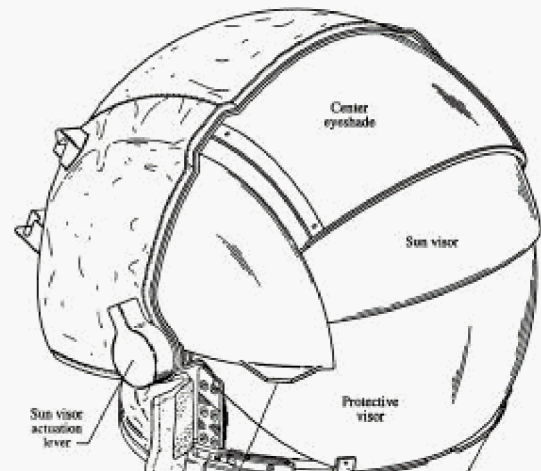


Figure 1-15. Illustration of the extravehicular visor assembly of the EMU showing protective visors and eyeshades. (Reproduced with permission from Hamilton Sundstrand.)

1.2.7 EMU Personal Life Support System

Due to its contents’ bulk, the PLSS (backpack) provides significant directional radiation shielding and scattering. It contains the primary water tanks, the silver-zinc EMU electricity battery, fans, pumps, a radio, and other equipment, including a metal oxide CO₂ sorbent canister that alone weighs 14.5 kg. To minimize corrosion, the ventilation subsystem and other components in the PLSS are composed of stainless steel (Fe, Cr, Ni) rather than aluminum.

1.2.8 Liquid Cooling Ventilation Garment

The LCVG covers the torso, arms, and legs to provide temperature regulation of the body. On Earth, it weighs ~3.5 kg dry, and holds 0.23 to 0.34 kg of water. The ethyl vinyl acetate cooling inlet/outlet tubes attached to

the MWC are approximately 8 mm, and the transport tubes sewn inside the garment are approximately 4 mm outer diameter, and 84 m in length. The areal density of the Spandex/Nylon fabric is 0.034 g cm^2 , and the transport tubes (see **Figure 1-12**) filled with water are 0.078 g cm^2 maximum. The nonuniformity of the LCVG shielding “shadow” at the skin is a topic of ongoing research (Anderson et al., 2001).

1.2.9 Orlan-M Space Suit

The Orlan-M (**Figures 1-16 and 1-17**) is one of many space suits designed and manufactured by Zvezda (“Star”) for the Russian space program since the mid-1960s. The “M” model was first tested and used to perform EVA aboard the *Mir* Space Station on 29 April, 1997; it was the 154th EVA, the 78th Russian/Soviet, and the 77th EVA for the United States (Portree and Treviño 1997). Within a year, the suit had been worn during a dozen EVAs.

The space suit body consists of an aluminum alloy torso and helmet of ~1.2 mm thickness and the arm and legs are

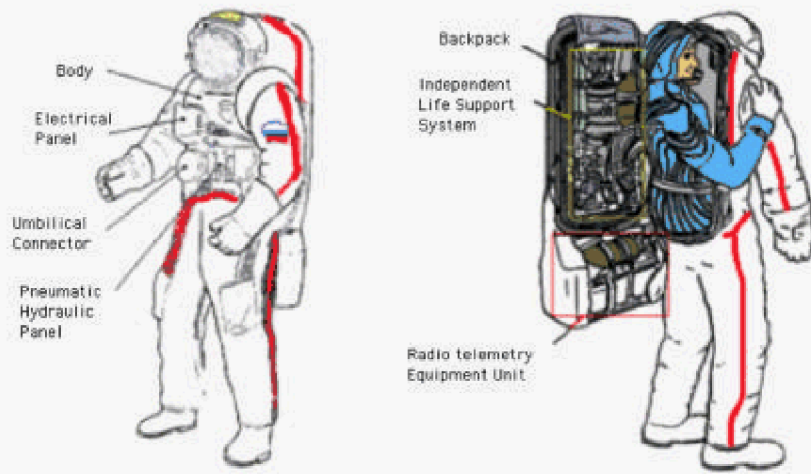


Figure 1-16. Illustration of the Orlan-M space suit (Anon., 1997).



Figure 1-17. Orlan-M EVA space suit used in experiments at Loma Linda University Medical Center.

soft shell. Unlike the EMU, both the helmet and life support backpack of the Orlan-M are integrated components of the suit. The wearer enters the suit from the rear through a hatch between the life-support backpack and the rigid body. The fabric layup is described in **Table 1-4**. The Orlan-M accommodates persons with chest circumference of 94-110 cm and standing height of 165-182 cm. The suit mass is no greater than 100 kg, and requires an external support structure for handling on Earth. (Unfortunately, the structure prevented some experimental procedures that were performed on the EMU.) The operating pressure is 40.7 kpascal (5.9 psi). Noticeable upgrades to the space suit from the earlier Orlan-DMA model include a second visor on top of the helmet and a functionally improved glove design. The underwear-coveralls are made of a cotton-knitted fabric. The cooling garment consists of ~60 m of water-filled tubes. The cooling garment completely filled with cooling liquid, together with the coverall, weighs less than 3 kg. However, these components were not available for testing.

Table 1-4. Orlan-M Suit Fabric Layup

Layer	Material	Comments
Protective garment	Phenilon	Nomex type
Radio-fabric	Capron & silver	Mesh type
PETF film	Polyethylene	Porous type
PETF film	Polyethylene	Reinforced porous
PETF film	Polyethylene	Porous type
PETF film	Polyethylene	Reinforced porous
PETF film	Polyethylene	Thick layer
Radio-fabric	Capron & silver	Mesh type
Lining	Capron	Nylon type
Restraint layer	LAVSAN (Polyethylene), Dacron	Thick cloth type
Primary bladder	Natural latex type	Rubber stretch type
Redundant bladder	Rubber-coated Capron	Metallic rubber
Lining	Capron	Nylon type
Liquid cooling garment	Spandex & Capron tricot	Porous stretch fabric
Inner garment		

1.2.10 Human Phantom

The Phantom Laboratory of Salem, New York, manufactured the anthropomorphic phantom used to simulate the astronaut body for the Loma Linda University (LLU) radiobiology program. The incomplete phantom, shown in **Figure 1-18**, is sized to the 50th percentile U.S. male anthropometry (Alderson 1962). The phantom is constructed with a human skeleton cast inside material with the mass density (1.002 g cm^3) and radiological equivalence (electron density) of soft tissue. Molded lungs fit the contours of human lungs in a median respiratory state within the natural human rib cage and are composed of low-density (0.305 g cm^3) polymeric foam. Phantoms are sliced into 2.5-cm-thick axial cross-sectional slices. In the space suit experiments performed at LLU reported herein, TLDs, solid-state silicon detectors, CR-39 plastic nuclear track detectors (PNTDs), and cell samples are placed outside the left eye and deep in the head and upper and lower abdomen.

Figure 1-18. Photograph of partial human phantom of tissue-equivalent material. Detectors and biological samples were irradiated at various positions inside the phantom. Large removable plugs are visible in the abdomen and right thigh.



1.3 REFERENCES

- Alderson, S. W., Lanzl, L. H., Rollins, M., Spira, J., 1962. An instrumented phantom system for analog computation of treatment plans. *The American J. of Roentgenology, Radium Therapy, and Nuclear Medicine*, Vol. 87(1), p185.
- Anderson, B. M.; Nealy, J. E.; Qualls, G. D., Staritz, P. J.; Wilson, J. W.; Kim, M.-H. Y., Cucinotta, F. A., Atwell, W., DeAngelis, G., Ware, J., Persans, A. E., 2001. Shuttle space suit (radiation) model development. Soc. Auto. Eng., Inc. SAE Paper 01ICES-2363.
- Anon., 1997. Orlan-M Extra-vehicular Activity Spacesuit Training Manual. Yu. A. Gagarin Cosmonaut Training Center. Publication 01.09.05.05(0)T0002, (English translation: SS1653/TTI/DG/GL/08/19/98).
- Anon, 1999. EMU system training workbook. NASA-Johnson Space Center publication JSC-19450, 2-49–2-55.
- Anon, 2000. NASA EMU LSS/SSA data book, Rev. F. Hamilton Standard, 451.
- Badhwar, G., 2000. Free space radiation environment. In: Fujitake, K.; Majima, H.; Ando, K.; Yasuda, H.; Suzuki, M. Risk evaluation of cosmic-ray exposure in long-term manned space mission. Proceedings of the International workshop on Responses to heavy particle radiation, Chiba, July 9–10, 1998. Kodansha Scientific, Ltd., Tokyo.
- Barth, J., 1996. Modeling space radiation environments. IEEE Short Course: Applying computer simulation tools to radiation effects problems. IEEE Publications Services, Piscataway, NJ.
- Benton, E. R., Benton, E. V., 1999. A survey of radiation measurements made aboard Russian spacecraft in low-earth orbit, NASA Contractor's Report–1999–209256, National Technical Information Service, Springfield, VA 22161.
- CFR, 2000. Code of Federal Regulations. Part 20—Standards for protection against radiation. Washington, DC: Office of the Federal Registrar, National Archives and Records Administration.
- Cucinotta, F. A., Schimmerling, W., Wilson, J. W., Peterson, L. E., Badhwar, G. D., Saganti, P., and Dicello, J. F. 2001a. Space radiation cancer risks and uncertainties for Mars missions. *Radiat. Res.* **156**: 682-688.
- Cucinotta, F. A., Manuel, F., Jones, J., Izsard, G., Murray, J., Djojonegoro, B., and Wear, M. 2001b. Space radiation and cataracts in astronauts. *Radiat. Res.* **156**: 460-466.
- Deme, S., Apathy, I., Hejja, I., Lang, E., Feher, I., 1999. Extra dose due to extravehicular activity during the NASA-4 mission measured by an on-board TLD system. *Rad. Prot. Dos.* 85(1-4):121-124.
- Gussenhoven, M. S. Mullen, E. G., Brautigam, D. H., 1996. Improved understanding of the Earth's radiation belts from the CRRES satellite. *IEEE Trans. on Nucl. Science* 43(2): 353-368.
- Golightly, M. J., Weyland, M. D.; Hardy, A. C., 1995. Radiation exposure to astronauts during EVAs. Soc. Auto. Eng. Warrendale, PA, SAE technical paper series 951593.
- Heckman, H. H. and Nakano G. H., 1965. Direct observation of mirroring protons in the South Atlantic anomaly. *Space Res.* 5:329.
- ICRP, 1991. International Commission on Radiological Protection. 1990 Recommendations of the International Commission on Radiological Protection, ICRP Publication 60. Oxford: Pergamon Press; Ann. ICRP 21(1-3).